Rate-Energy Tradeoff in Simultaneous Wireless Information and Power Transfer over Fading Channels with Uncertain Distribution

Qi Gu, Gongpu Wang, Rongfei Fan, Zhangdui Zhong, Kai Yang, and Hai Jiang

***Abstract*—This paper investigates the tradeoff between information rate and harvested energy in a simultaneous wireless information and power transfer system (SWIPT) under power splitting (PS) scheme and time switching (TS) scheme. A single-input-multiple-output (SIMO) transmitter-receiver pair is considered. For the channel from the transmitter to the receiver, only the mean and covariance matrix are known, but the instantaneous channel information or the channel gain distribution is unknown. We define robust outage capacity that applies for all possible channel distributions with the given mean and covariance matrix, and study the tradeoff between the robust outage capacity and harvested power level. By solving optimization problems, we find the PS ratio setting for PS scheme and TS ratio setting for TS scheme to achieve the outer boundary of robust outage capacity-energy region (which includes all possible pairs of achievable robust outage capacity and harvested power level). The PS and TS ratio setting are fixed over fading blocks, and thus, can avoid communication overhead and computation overhead over each fading block, and facilitate a simple implementation in a practical system. We also prove that the robust outage capacity-energy regions in PS scheme and TS scheme are both convex. Further, we prove that the PS scheme outperforms the TS scheme in terms of the rate-energy tradeoff. Numerical results are also presented to verify the correctness of our theoretical results.**

***Index Terms*—Energy harvesting, rate-energy region, simultaneous wireless information and power transfer, outage capacity.**

I. Introduction

Simultaneous wireless information and power transfer (SWIPT) is a promising technology for energy-constrained wireless networks, which allows wireless terminals to use radio frequency (RF) signals to simultaneously transmit wireless power (for receivers to perform energy harvesting [EH]) and information signals (for receivers to perform information decoding [ID]). To achieve SWIPT, power splitting (PS) and time switching (TS) are two practical receiver designs [1]. In a PS scheme, the receiver splits the received RF signals to two parts, for energy harvesting and for information decoding, respectively. In a TS scheme, energy harvesting and information decoding are performed in different time portions at the receiver. For PS scheme (or TS scheme), if we allocate more power (or time) portion, called PS ratio (or TS ratio), for information decoding, the receiver can achieve a larger information rate, at the cost of a lower level of harvested power. Thus, in SWIPT, a tradeoff exists between information rate and harvested power, referred to as *rate-energy tradeoff*. In an X-Y plane, the *rate-energy region* of a SWIPT system is defined as the region that includes all possible pairs of achievable information rate and harvested power level. The outer boundary of the rate-energy region can be found by finding the maximal harvested power level for any given information rate, or by finding the maximal information rate for any given harvested power level. The outer boundary can clearly demonstrate the rate-energy tradeoff [2].

The issue of rate-energy tradeoff in SWIPT systems has been investigated in the literature, with focuses on achieving the outer boundary of rate-energy region by performing resource allocation and on investigating the shape of rate-energy region. For a single-input-single-output (SISO) system, the work in [3] considers the symbol training phase and data transmission phase in a PS scheme and derives optimal PS ratio for both phases. For SISO with TS and PS scheme, the work in [4] and the work in [5] maximize the ergodic capacity over fading channels, by finding the optimal transmission power as well as TS and PS ratio, respectively. The shape of rate-energy region of a SISO system with PS and TS scheme is investigated in [2] (which uses channel capacity to represent information rate) and [6] (which considers M-array modulation rate as information rate). For a single-input-multiple-output (SIMO) system with a PS scheme, the work in [7] derives the optimal PS ratio, and the work in [5] studies ergodic capacity maximization by optimal setting of transmission power and PS ratio. For a multiple-input-multiple-output (MIMO) system, the works in [8] and [9] study the precoder design for both PS and TS schemes, and the work in [10] considers nonlinearity of the energy harvesting process and jointly designs the precoder and the PS ratio for a PS scheme (or the TS ratio for a TS scheme). For a multiple-user system with a single-antenna transmitter and multiple single-antenna receivers, the work in [11] designs the optimal time and power allocation over multiple slots as well as the switching rule over each slot.

In the above works, to achieve optimal resource allocation (e.g., transmission power or precoding matrix design) and system parameter configuration (e.g., PS ratio and TS ratio), accurate and timely channel state information (CSI) in every fading block is assumed. This may be costly to achieve in a real network, as communication overhead (such as training sequence and feedback between the transmitter and the receiver) is required. Further, inaccurate instantaneous CSI may degrade the system performance.

In this paper, we investigate the rate-energy tradeoff without instantaneous CSI knowledge in every fading block. Specifically, we consider a SIMO system in which only mean and covariance matrix of the channel gains are known, but the instantaneous CSI or channel gain distribution is unknown. We find the optimal PS ratio and optimal TS ratio for a PS and TS scheme, respectively. Our PS and TS ratio are

 Manuscript received Feb. 25, 2017; revised Sep. 6, 2017; accepted Nov. 26, 2017. This work was supported in part by National Natural Science Foundation of China under Grant 61601025, Grant 61771054, Grant 61421001, Grant 61501028, and the Fundamental Research Funds for the Central Universities under Grant 2017YJS041. The review of this paper was coordinated by Dr. Oliver Holland. Corresponding author: Rongfei Fan (fanrongfei@bit.edu.cn).

Q. Gu and G. Wang are with Beijing Key Lab of Transportation Data Analysis and Mining, School of Computer and Information Technology, Beijing Jiaotong University, Beijing 100044, P. R. China (email:{15112094, gpwang}@bjtu.edu.cn). R. Fan and K. Yang are with the School of Information and Electronics, Beijing Institute of Technology, Beijing 100081, P. R. China (email:fanrongfei@bit.edu.cn,yangkai@ieee.org). Z. Zhong is with the State Key Laboratory of Rail Traffic Control and Safety, Beijing Jiaotong University, Beijing, China, 100044 (email:zhdzhong@bjtu.edu.cn). H. Jiang is with the Department of Electrical & Computer Engineering, University of Alberta, Edmonton, Alberta, Canada T6G 1H9 (e-mail: hai1@ualberta.ca).

robust in the following sense: i) They can guarantee an outage capacity for whatever channel gain distribution with the given mean and covariance matrix; ii) Since instantaneous CSI is not needed, our work is robust to inaccurate instantaneous CSI that happens in other existing works. Other benefits of our robust setting include: i) the communication overhead to get the instantaneous CSI is avoided; ii) the PS and TS ratio are fixed as long as the channel mean and covariance matrix do not change, which avoids computation overhead in each fading block and also facilitates a simple implementation of PS and TS scheme in a practical system (i.e., we do not need to adapt the PS and TS ratio frequently).[1] The contributions of this work are summarized as follows. 1) We formulate optimization problems to achieve the outer boundary of the robust outage capacity-energy region for PS and TS schemes (the definition of robust outage capacity is given in Section II), and by using some mathematical manipulations, we transform the formulated problems to convex problems; 2) We prove the convexity of the robust outage capacity-energy regions in the PS and TS schemes; 3) We theoretically prove that the PS scheme achieves a better performance than the TS scheme.

II. System Model

Consider a point-to-point SWIPT SIMO system, in which the transmitter is equipped with a single antenna and the receiver is equipped with N antennas denoted as $1, 2, ..., N$, respectively.[2] The transmission power of the transmitter is P. The channel gains between the transmitter and the N antennas at the receiver are denoted as $h_1, h_2, ..., h_N$, respectively. Block fading is assumed, i.e., $h_1, h_2, ..., h_N$ keep unchanged within a time slot (a fading block), and may change independently across time slots. Denote $\boldsymbol{h} = (h_1, h_2, ..., h_N)^T$, where $(\cdot)^T$ means transpose operation. Neither the transmitter nor the receiver knows $\boldsymbol{h}$ in every fading block. Denote the probability density function (PDF) of $\boldsymbol{h}$ as $f(\boldsymbol{h})$, which is unknown. Mean and covariance matrix of $\boldsymbol{h}$ are known, expressed as $\boldsymbol{\mu} = (\mu_1, \mu_2, ..., \mu_N)^T$ and $\mathbf{C}$, respectively.[3] Each antenna at the receiver experiences circularly symmetric complex Gaussian (CSCG) noise with zero mean and variance σ^2.

[1] As a popular robust optimization method, the Ben-Tal's approach [12] can be used to deal with channel estimation uncertainty by assuming that 1) the channel estimation error is always within a predefined region, or 2) the channel estimation error's probability density function (PDF) is known. When the Ben-Tal's approach is applied in our system, channel estimation is needed. Different from the Ben-Tal's approach, in this paper, we deal with uncertainty of channel estimation from another perspective: we eliminate the process of channel estimation (and thus, we do not need to reserve some time portion in each time slot for channel estimation), and investigate the outage capacity.

[2] Here we consider multiple antennas at the receiver as more energy can be harvested from multiple antennas. On the other hand, we do not consider multiple antennas at the transmitter. This is because the focus of this paper is to characterize the impact of PS/TS ratio and find out insights, while including multiple antennas at the transmitter will lead to a problem of joint PS/TS ratio setting and precoder design at the multiple transmitter antennas. As the first research that deals with the tradeoff between robust outage capacity and energy, we select a SIMO model and focus on optimal PS/TS ratio setting. A MIMO case can be treated as follows. Different from our SIMO case where the non-closed-form robust outage capacity constraints (2) and (4) can be transformed to closed-form constraints, the MIMO-version robust outage capacity constraints are difficult to be transformed to closed-form ones, and thus, the research problem is difficult to solve. A method could be to select the transmitter antenna with the best performance, and thus, the research problem is simplified to the SIMO case problem.

[3] The motivation for this setting is as follows. It may be difficult to get the accurate distribution for a practical wireless channel. Rather, it is not difficult to get the mean and covariance matrix, for example, by using sampling.

In PS scheme, for antenna $n \in \{1, 2, ..., N\}$, denote the portion of received signal used for ID and EH as α_n and $(1-\alpha_n)$, respectively. Note that to achieve the maximal flexibility and maximal utility, α_n can be different from each other. In addition, uniform α_n will lead to less utility, which will be shown in (22). Define $\boldsymbol{\alpha} = (\alpha_1, \alpha_2, ..., \alpha_N)^T$.

Since instantaneous CSI is not assumed, transmission outage may happen, and we focus on outage capacity. According to [13], the outage capacity is the maximal R such that the probability that the channel capacity falls below R is not more than a predefined threshold ε, expressed as

$$\Pr\left(\log_2\left(1 + \frac{P \cdot \boldsymbol{\alpha}^T \boldsymbol{h}}{\sigma^2}\right) \leq R\right) \leq \varepsilon, \tag{1}$$

in which $\Pr(\cdot)$ means probability. To evaluate the left-hand side of (1), information of $f(\boldsymbol{h})$ (PDF of $\boldsymbol{h}$) is necessary. However, as we do not know $f(\boldsymbol{h})$, and we only know the mean and covariance matrix of $\boldsymbol{h}$, we focus on *robust outage capacity*, defined as the maximal R_p [4] such that, for whatever channel PDF $f(\boldsymbol{h})$, as long as the mean and covariance matrix of $\boldsymbol{h}$ are $\boldsymbol{\mu}$ and $\mathbf{C}$, respectively, the probability that the channel capacity falls below R_p is not more than a predefined threshold ε. Mathematically, denote $D(\boldsymbol{h}) = \{f(\boldsymbol{h}) | \mathbb{E}_{f(\boldsymbol{h})}\{\boldsymbol{h}\} = \boldsymbol{\mu}, \mathbb{E}_{f(\boldsymbol{h})}\left\{(\boldsymbol{h}-\boldsymbol{\mu})(\boldsymbol{h}-\boldsymbol{\mu})^T\right\} = \mathbf{C}\}$ as the set of all possible $f(\boldsymbol{h})$ whose mean is equal to $\boldsymbol{\mu}$ and whole covariance matrix is the same as $\mathbf{C}$, where $\mathbb{E}_{f(\boldsymbol{h})}\{\cdot\}$ means expectation over variable $\boldsymbol{h}$ with PDF $f(\boldsymbol{h})$. Then we have

$$\sup_{f(\boldsymbol{h}) \in D(\boldsymbol{h})} \Pr\left(\log_2\left(1 + \frac{P \cdot \boldsymbol{\alpha}^T \boldsymbol{h}}{\sigma^2}\right) \leq R_p\right) \leq \varepsilon. \tag{2}$$

For EH in PS scheme, according to [2], the average harvested power is expressed as

$$\gamma_p = \eta P \cdot (\mathbf{1} - \boldsymbol{\alpha})^T \boldsymbol{\mu} \tag{3}$$

in which $\eta \in (0, 1)$ is the energy conversion efficiency.

In TS scheme, at the transmitter side, portion $(1-\beta)$ of each time slot is used for EH purpose, and portion β of each time slot is used for ID purpose. Thus, all the antennas at the receiver should be synchronized to this setting, i.e., perform EH within time portion $(1-\beta)$, and perform ID within time portion β. Similar to the PS scheme, the robust outage capacity of TS scheme, denoted as R_t in which the subscript t means "time switching," satisfies

$$\sup_{f(\boldsymbol{h}) \in D(\boldsymbol{h})} \Pr\left(\beta \log_2\left(1 + \frac{P \cdot \mathbf{1}^T \boldsymbol{h}}{\sigma^2}\right) \leq R_t\right) \leq \varepsilon \tag{4}$$

in which $\mathbf{1}$ is a vertical vector with all N elements equal to 1. And the average harvested power in TS scheme is expressed as [2]

$$\gamma_t = \eta P (1-\beta) \cdot \mathbf{1}^T \boldsymbol{\mu}. \tag{5}$$

III. Tradeoff between Robust Outage Capacity and Average Harvested Power

A. Problem Formulation and Transformation

According to [2], the robust outage capacity-energy region for PS scheme and TS scheme can be given as

$$\mathcal{R}_p = \bigcup_{\boldsymbol{\alpha}, \mathbf{0} \preceq \boldsymbol{\alpha} \preceq \mathbf{1}} \{(R, \gamma) | R \leq R_p, \gamma \leq \gamma_p\} \tag{6}$$

[4] Here the subscript 'p' denotes "power splitting".

and

$$\mathcal{R}_t = \bigcup_{\beta, 0 \le \beta \le 1} \left\{ (R, \gamma) | R \le R_t, \gamma \le \gamma_t \right\}, \tag{7}$$

respectively, in which $\mathbf{0}$ is a vertical vector whose all N elements are equal to 0. The outer boundary of $\mathcal{R}_p$ and $\mathcal{R}_t$ define the limit of EH and ID capability under PS scheme and TS scheme, respectively. To achieve the outer boundary of $\mathcal{R}_p$ (or $\mathcal{R}_t$), γ_p in PS scheme (or γ_t in TS scheme) should be maximized for given R_p (or R_t). Specifically, the following optimization problem should be solved for a given R_p under PS scheme[5]

Problem 1:

$$\begin{aligned} \max_{\boldsymbol{\alpha}} \quad & \eta P \cdot (\mathbf{1} - \boldsymbol{\alpha})^T \boldsymbol{\mu} \\ \text{s.t.} \quad & \mathbf{0} \preceq \boldsymbol{\alpha} \preceq \mathbf{1}, \\ & \text{Constraint } (2), \end{aligned} \tag{8}$$

and the following optimization problem should be solved for a given R_t under TS scheme

Problem 2:

$$\begin{aligned} \max_{\beta} \quad & \eta P (1 - \beta) \cdot \mathbf{1}^T \boldsymbol{\mu} \\ \text{s.t.} \quad & 0 \le \beta \le 1, \\ & \text{Constraint } (4) \,. \end{aligned} \tag{9}$$

It can be seen that the constraints (2) and (4) are not in closed-form, which makes Problem 1 and Problem 2 hard to solve. The following lemma shows how to transform the non-closed-form constraints to equivalent closed-form expressions.

Lemma 1: The constrains (2) and (4) are equivalent to

$$\boldsymbol{\alpha}^T \boldsymbol{\mu} - \sqrt{\frac{1}{\varepsilon} - 1} \cdot \sqrt{\boldsymbol{\alpha}^T \mathbf{C} \boldsymbol{\alpha}} \ge \frac{\sigma^2}{P} \left(2^{R_p} - 1 \right) \tag{10}$$

and

$$\beta \ge \frac{R_t}{\log_2 \left(1 + \frac{P}{\sigma^2} \left(\mathbf{1}^T \boldsymbol{\mu} - \sqrt{\frac{1}{\varepsilon} - 1} \cdot \sqrt{\mathbf{1}^T \mathbf{C} \mathbf{1}} \right) \right)}, \tag{11}$$

respectively.

Proof: We first show the equivalence between constraint (2) and constraint (10). Constraint (2) can be rewritten as

$$\sup_{f(\boldsymbol{h}) \in D(\boldsymbol{h})} \Pr \left(\boldsymbol{\alpha}^T \boldsymbol{h} \le \frac{(2^{R_p} - 1)\sigma^2}{P} \right) \le \varepsilon. \tag{12}$$

According to [14, Theorem 3.3], the left-hand side of (12) can be written as

$$\frac{\boldsymbol{\alpha}^T \mathbf{C} \boldsymbol{\alpha}}{\boldsymbol{\alpha}^T \mathbf{C} \boldsymbol{\alpha} + \left(\boldsymbol{\alpha}^T \boldsymbol{\mu} - \frac{\sigma^2}{P} \left(2^{R_p} - 1 \right) \right)^2} \tag{13}$$

when $\boldsymbol{\alpha}^T \boldsymbol{\mu} \ge \left(\sigma^2 / P \right) \left(2^{R_p} - 1 \right)$.[6] Substituting the left-hand side of (12) with the term in (13) and after some mathematical manipulations, constraint (12) can be transformed equivalently to (10).

By using the same method, constraint (4) can be proved to be equivalent to (11). For brevity, the proof is omitted. ■

According to Lemma 1, by replacing constraint (2) with constraint (10), replacing constraint (4) with constraint (11), and omitting the constant coefficient ηP in the objective function, Problem 1 can be rewritten as

Problem 3:

$$\begin{aligned} W(R_p, \varepsilon) \triangleq \max_{\boldsymbol{\alpha}} \quad & (\mathbf{1} - \boldsymbol{\alpha})^T \boldsymbol{\mu} \\ \text{s.t.} \quad & \mathbf{0} \preceq \boldsymbol{\alpha} \preceq \mathbf{1}, & \text{(14a)} \\ & \text{Constraint (10)}, & \text{(14b)} \end{aligned}$$

and Problem 2 is equivalent to

Problem 4:

$$\begin{aligned} Z(R_t, \varepsilon) \triangleq \max_{\beta} \quad & (1 - \beta) \cdot \mathbf{1}^T \boldsymbol{\mu} \\ \text{s.t.} \quad & 0 \le \beta \le 1, \\ & \text{Constraint (11)}. \end{aligned}$$

Both Problem 3 and Problem 4 are convex problems.

In the following, we present special features of the two problems. For presentation simplicity, we omit the subscript of R_p and R_t in $W(R_p, \varepsilon)$ and $Z(R_t, \varepsilon)$, respectively, and thus, $W(R_p, \varepsilon)$ and $Z(R_t, \varepsilon)$ are written as $W(R, \varepsilon)$ and $Z(R, \varepsilon)$, respectively.

B. Analytical Results of $W(R, \varepsilon)$ and $Z(R, \varepsilon)$

For the PS scheme, the function $W(R, \varepsilon)$ defined in Problem 3 has the following feature.

Theorem 1: $W(R, \varepsilon)$ is non-increasing and concave with R for a given ε, and is non-decreasing with ε for a given R.

Proof: We first prove $W(R, \varepsilon)$ is concave with R for given ε. For two specific R values: $R^\dagger$ and $R^\ddagger$, assume the vectors $\boldsymbol{\alpha}$ achieving $W(R^\dagger, \varepsilon)$ and $W(R^\ddagger, \varepsilon)$ are $\boldsymbol{\alpha}^\dagger = \left(\alpha_1^\dagger, \alpha_2^\dagger, ..., \alpha_N^\dagger \right)^T$ and $\boldsymbol{\alpha}^\ddagger = \left(\alpha_1^\ddagger, \alpha_2^\ddagger, ..., \alpha_N^\ddagger \right)^T$, respectively. Then $W(R^\dagger, \varepsilon) = \sum_{n=1}^N \left(1 - \alpha_n^\dagger \right) \mu_n$ and $W(R^\ddagger, \varepsilon) = \sum_{n=1}^N \left(1 - \alpha_n^\ddagger \right) \mu_n$. For vector $\boldsymbol{\alpha}$ taking a new specific value equal to $\left(\theta \boldsymbol{\alpha}^\dagger + (1 - \theta) \boldsymbol{\alpha}^\ddagger \right)$ with $\theta \in (0, 1)$, we have

$$\begin{aligned} & \left(\theta \boldsymbol{\alpha}^\dagger + (1 - \theta) \boldsymbol{\alpha}^\ddagger \right)^T \boldsymbol{\mu} \\ & - \sqrt{\tfrac{1}{\varepsilon} - 1} \cdot \sqrt{\left(\theta \boldsymbol{\alpha}^\dagger + (1 - \theta) \boldsymbol{\alpha}^\ddagger \right)^T \mathbf{C} \left(\theta \boldsymbol{\alpha}^\dagger + (1 - \theta) \boldsymbol{\alpha}^\ddagger \right)} \\ \overset{\text{(a)}}{\ge} \; & \left(\theta \boldsymbol{\alpha}^\dagger + (1 - \theta) \boldsymbol{\alpha}^\ddagger \right)^T \boldsymbol{\mu} \\ & - \sqrt{\tfrac{1}{\varepsilon} - 1} \cdot \left(\theta \sqrt{(\boldsymbol{\alpha}^\dagger)^T \mathbf{C} \boldsymbol{\alpha}^\dagger} + (1 - \theta) \sqrt{(\boldsymbol{\alpha}^\ddagger)^T \mathbf{C} \boldsymbol{\alpha}^\ddagger} \right) \\ \overset{\text{(b)}}{\ge} \; & \tfrac{\sigma^2}{P} \left(\left(\theta 2^{R^\dagger} + (1 - \theta) 2^{R^\ddagger} \right) - 1 \right) \\ \overset{\text{(c)}}{\ge} \; & \tfrac{\sigma^2}{P} \left(2^{\left(\theta R^\dagger + (1 - \theta) R^\ddagger \right)} - 1 \right) \end{aligned} \tag{16}$$

where (a) comes from the convexity of function $\sqrt{\boldsymbol{\alpha}^T \mathbf{C} \boldsymbol{\alpha}}$ with $\boldsymbol{\alpha}$, (b) holds since $\boldsymbol{\alpha}^\dagger$ and $\boldsymbol{\alpha}^\ddagger$ satisfy constraint (14b) for $R_p = R^\dagger$ and $R_p = R^\ddagger$, respectively, and (c) is due to the convexity of function 2^R with R. Inequality (16) shows that $\left(\theta \boldsymbol{\alpha}^\dagger + (1 - \theta) \boldsymbol{\alpha}^\ddagger \right)$ satisfies constraint (14b) for $R_p = (\theta R^\dagger + (1 - \theta) R^\ddagger)$, and thus, is a feasible point of Problem 3 when $R_p = (\theta R^\dagger + (1 - \theta) R^\ddagger)$, with corresponding objective function of Problem 3 given as $\left(\mathbf{1} - \left(\theta \boldsymbol{\alpha}^\dagger + (1 - \theta) \boldsymbol{\alpha}^\ddagger \right) \right)^T \boldsymbol{\mu}$. Apparently, this objective function is not more than $W \left(\left(\theta R^\dagger + (1 - \theta) R^\ddagger \right), \varepsilon \right)$, the maximal

[5] For any specific R_p, by solving Problem 1 we can get the optimal vector $\boldsymbol{\alpha}$ and maximal average harvested power γ_p. The pair (R_p, γ_p) corresponds to one point on the outer boundary of $\mathcal{R}_p$, and can be achieved by the optimal vector $\boldsymbol{\alpha}$. By varying the specific R_p value, we can get the whole outer boundary of $\mathcal{R}_p$. The case with the TS scheme can be treated similarly.

[6] When $\boldsymbol{\alpha}^T \boldsymbol{\mu} < \frac{\sigma^2}{P} \left(2^{R_p} - 1 \right)$, the left-hand side of constraint (12) is equal to 1 and thus, constraint (12) never holds since $\varepsilon < 1$.

objective function of Problem 3 when $R_p = (\theta R^\dagger + (1-\theta)R^\ddagger)$. Then, we have

$$\begin{aligned} W\left(\left(\theta R^\dagger + (1-\theta)R^\ddagger\right), \varepsilon\right) \geq \left(\mathbf{1} - \left(\theta \boldsymbol{\alpha}^\dagger + (1-\theta)\,\boldsymbol{\alpha}^\ddagger\right)\right)^T \boldsymbol{\mu} \\ = \theta W(R^\dagger, \varepsilon) + (1-\theta) W(R^\ddagger, \varepsilon), \end{aligned} \quad (17)$$

which shows the concavity of function $W(R,\varepsilon)$ with R for given ε.

Next we prove that $W(R,\varepsilon)$ is non-increasing with R. It can be checked that when R increases, the feasible region of Problem 3 shrinks according to (14b), and thus, Problem 3 cannot achieve a higher objective function. Therefore, function $W(R,\varepsilon)$ is non-increasing with R for a given ε.

Similarly, for a given R, when ε increases, the feasible region of Problem 3 is enlarged. Thus, function $W(R,\varepsilon)$ is non-decreasing with ε for a given R. ■

Remark: Theorem 1 shows that for a given ε, region $\mathcal{R}_p$ (robust outage capacity-energy region for PS scheme) is convex, since the outer boundary of $\mathcal{R}_p$, which is represented by $W(R,\varepsilon)$, is non-increasing and concave when R grows.

Next we analyze function $Z(R,\varepsilon)$ for Problem 4 for TS scheme. For a given ε, denote β^* as the optimal β that achieves $Z(R,\varepsilon)$ (i.e., the optimal point of Problem 4).

Define $U(\varepsilon) = \left(\frac{P}{\sigma^2}\right)\left(\mathbf{1}^T\boldsymbol{\mu} - \sqrt{\left(\frac{1}{\varepsilon}\right) - 1} \cdot \sqrt{\mathbf{1}^T\mathbf{C}\mathbf{1}}\right)$. Then constraint (11) can be re-written as

$$\beta \geq \frac{R}{\log_2\left(1 + U(\varepsilon)\right)}. \quad (18)$$

When $U(\varepsilon) \geq \left(2^R - 1\right)$, we have $\left(\frac{R}{\log_2(1+U(\varepsilon))}\right) \leq 1$. Thus, the feasible region of Problem 4 is $\beta \in [\frac{R}{\log_2(1+U(\varepsilon))}, 1]$ according to (18), and we can get

$$\beta^* = \frac{R}{\log_2\left(1 + U(\varepsilon)\right)} \quad (19)$$

and $Z(R,\varepsilon) = \left(1 - \frac{R}{\log_2(1+U(\varepsilon))}\right)\mathbf{1}^T\boldsymbol{\mu}$. Note that if $U(\varepsilon) = \left(2^R - 1\right)$, $Z(R,\varepsilon) = 0$.

When $U(\varepsilon) < \left(2^R - 1\right)$, we have $\left(\frac{R}{\log_2(1+U(\varepsilon))}\right) > 1$, and Problem 4 becomes infeasible according to (18) (noting that we require $\beta \in [0,1]$). In this case, we can write $Z(R,\varepsilon) = 0$.

In summary, for Problem 4, we have

$$Z(R,\varepsilon) = \begin{cases} \left(1 - \frac{R}{\log_2(1+U(\varepsilon))}\right)\mathbf{1}^T\boldsymbol{\mu}, & \text{if } U(\varepsilon) > \left(2^R - 1\right) \\ 0, & \text{if } U(\varepsilon) \leq \left(2^R - 1\right). \end{cases} \quad (20)$$

The following theorem is in order.

Theorem 2: for Problem 4, when $Z(R,\varepsilon) > 0$,

- $Z(R,\varepsilon)$ is linearly decreasing with R for a given ε.
- $Z(R,\varepsilon)$ is monotonically increasing with ε for a given R.

Proof: When $Z(R,\varepsilon) > 0$, we have $U(R,\varepsilon) > \left(2^R - 1\right)$, and from (20) we have $Z(R,\varepsilon) = \left(1 - \left(\frac{R}{\log_2(1+U(\varepsilon))}\right)\right)\mathbf{1}^T\boldsymbol{\mu}$, from which it can be seen that 1) $Z(R,\varepsilon)$ is linearly decreasing with R for given ε, and 2) $Z(R,\varepsilon)$ is monotonically increasing with ε for a given R since the function $U(\varepsilon)$ is an increasing function with ε. ■

Remark: Theorem 2 shows that, for a given ε, the region $\mathcal{R}_t$ (robust outage capacity-energy region for TS scheme) is convex and has a shape of triangle, since the outer boundary of region $\mathcal{R}_t$, which is represented by $Z(R,\varepsilon)$, is a linear decreasing function with R.

C. Comparison between $W(R,\varepsilon)$ and $Z(R,\varepsilon)$

In this subsection, we compare $W(R,\varepsilon)$ and $Z(R,\varepsilon)$. Specifically, the following theorem can be expected.

Theorem 3: Given ε fixed, $W(R,\varepsilon) \geq Z(R,\varepsilon)$ for any R.

Proof: We first consider adding an additional constraint $\alpha_1 = \alpha_2 = ... = \alpha_N = \alpha$ to Problem 3. The additional constraint means that all the antennas at the receiver use the same PS ratio for information decoding. With the additional constraint, Problem 3 becomes

Problem 5:

$$\begin{aligned} V(R,\varepsilon) \triangleq \max_{\alpha} \quad & (1-\alpha)\cdot\mathbf{1}^T\boldsymbol{\mu} \\ \text{s.t.} \quad & 0 \leq \alpha \leq 1, && (21a) \\ & \alpha \geq \tfrac{2^R - 1}{U(\varepsilon)} && (21b) \end{aligned}$$

in which constraint (21b) is from constraint (10) together with the additional constraint $\alpha_1 = \alpha_2 = ... = \alpha_N = \alpha$.

Apparently we have

$$W(R,\varepsilon) \geq V(R,\varepsilon) \quad (22)$$

because Problem 5 imposes an additional constraint on Problem 3. Similar to the derivation of (20), we have

$$V(R,\varepsilon) = \begin{cases} \left(1 - \left(\frac{2^R-1}{U(\varepsilon)}\right)\right)\mathbf{1}^T\boldsymbol{\mu}, & \text{if } U(\varepsilon) > \left(2^R - 1\right) \\ 0, & \text{if } U(\varepsilon) \leq \left(2^R - 1\right). \end{cases} \quad (23)$$

Next we prove that $V(R,\varepsilon) \geq Z(R,\varepsilon)$. We first consider the case that $U(\varepsilon) \leq \left(2^R - 1\right)$. In this case, from (20) and (23), we have $V(R,\varepsilon) = Z(R,\varepsilon) = 0$.

In the following, we consider the case that $U(\varepsilon) > \left(2^R - 1\right)$. In this case, from (20) and (23), we have

$$Z(R,\varepsilon) = \left(1 - \left(\frac{R}{\log_2\left(1 + U\left(\varepsilon\right)\right)}\right)\right)\mathbf{1}^T\boldsymbol{\mu}, \quad (24)$$

$$V(R,\varepsilon) = \left(1 - \left(\frac{\left(2^R - 1\right)}{U(\varepsilon)}\right)\right)\mathbf{1}^T\boldsymbol{\mu}. \quad (25)$$

For Problem 4, we already derived (19). We have the following equivalent expressions for (19).

$$\begin{aligned} & \beta^* = \tfrac{R}{\log_2(1+U(\varepsilon))} \Longleftrightarrow 1 = \tfrac{\left(2^{\frac{R}{\beta^*}} - 1\right)}{U(\varepsilon)} \Longleftrightarrow \\ & \beta^* = \tfrac{\beta^*\left(2^{\frac{R}{\beta^*}} - 1\right)}{U(\varepsilon)} \Longleftrightarrow \tfrac{R}{\log_2(1+U(\varepsilon))} = \tfrac{\beta^*\left(2^{\frac{R}{\beta^*}} - 1\right)}{U(\varepsilon)}. \end{aligned} \quad (26)$$

Using the last equivalent expression, $Z(R,\varepsilon)$ in (24) can be re-written as

$$Z(R,\varepsilon) = \left(1 - \frac{\beta^*\left(2^{R/\beta^*} - 1\right)}{U(\varepsilon)}\right)\mathbf{1}^T\boldsymbol{\mu}. \quad (27)$$

From (25) and (27), to prove $V(R,\varepsilon) \geq Z(R,\varepsilon)$, it suffices if we prove $H(\beta^*, R) \geq 0$, where $H(\beta, R) \triangleq \beta(2^{R/\beta} - 1) - (2^R - 1)$.

Looking into $H(\beta,R)$, we have $\frac{\partial H(\beta,R)}{\partial \beta} = -1 + \frac{\left(2^{R/\beta}(\beta - R\ln(2))\right)}{\beta}$ and $\frac{\partial^2 H(\beta,R)}{\partial^2 \beta} = \frac{\left(R^2\ln^2(2)2^{R/\beta}\right)}{\beta^3} \geq 0$. As $\frac{\partial^2 H(\beta,R)}{\partial^2 \beta} \geq 0$, $\frac{\partial H(\beta,R)}{\partial \beta}$ is increasing with β. When $\beta = 1$, define $y(R) \triangleq \frac{\partial H(\beta,R)}{\partial \beta}|_{\beta=1} = -1 + 2^R\left(1 - R\ln(2)\right)$. Then we have $\frac{\partial y(R)}{\partial R} = -2^R R\ln^2(2) \leq 0$, which indicates that $y(R)$ is a decreasing function with R. Since it can be easily checked that $y(R)|_{R=0} = 0$, we have $y(R) \leq 0$ when

$R \geq 0$. In other words, $\frac{\partial H(\beta,R)}{\partial \beta}|_{\beta=1} \leq 0$ since R always satisfies $R \geq 0$. Combining with the fact that $\frac{\partial H(\beta,R)}{\partial \beta}$ is increasing with β, we have $\frac{\partial H(\beta,R)}{\partial \beta} \leq 0$ when β lies in $[0,1]$, which means that $H(\beta,R)$ is a non-increasing function with $\beta \in [0,1]$. Together with the fact that $H(\beta,R)|_{\beta=1} = 0$, it can be concluded that $H(\beta,R) \geq 0$ for $\beta \in [0,1]$. Since $\beta^* = \frac{R}{\log_2(1+U(\varepsilon))} \in (0,1)$, we have $H(\beta^*,R) \geq 0$. This completes the proof for $V(R,\varepsilon) \geq Z(R,\varepsilon)$.

Combining the fact that $V(R,\varepsilon) \geq Z(R,\varepsilon)$ and $W(R,\varepsilon) \geq V(R,\varepsilon)$ in (22), we have $W(R,\varepsilon) \geq Z(R,\varepsilon)$. ■

Remark: Theorem 3 implies that, for a given ε, we have $\mathcal{R}_p \supseteq \mathcal{R}_t$ since the outer boundary of $\mathcal{R}_p$ (represented by $\eta PW(R,\varepsilon)$) is not smaller than the outer boundary of $\mathcal{R}_t$ (represented by $\eta PZ(R,\varepsilon)$). Theorem 3 also indicates that PS scheme can achieve better performance than TS scheme.

IV. Numerical Results

Here numerical results are presented. Consider the number of antennas at the receiver as $N = 3$, and the outage probability as $\varepsilon = 0.1$ (unless otherwise specified). Similar to [2], the transmission power is $P = 1$ W (unless otherwise specified), noise variance σ^2 is -70 dBmW, the carrier frequency is 900 MHz, the radio signal bandwidth is 10 MHz, the energy conversion efficiency is $\eta = 0.5$, and the distance between the transmitter and receiver is 1 m. The wireless channel experiences free space path loss and Nakagami fading, and accordingly, the channel gain is Gamma distributed, with shape parameter and scale parameter set as 10 and 0.1, respectively. The channel's mean vector and covariance matrix are estimated from 1000 channel gain realizations.

Fig. 1 plots $\eta PW(R,\varepsilon)$ (average harvested power in PS scheme) and $\eta PZ(R,\varepsilon)$ (average harvested power in TS scheme) under different transmission power P. The regions under the $\eta PW(R,\varepsilon)$ and $\eta PZ(R,\varepsilon)$ curves are the robust outage capacity-energy regions $\mathcal{R}_p$ and $\mathcal{R}_t$, respectively. It can be seen that $\eta PW(R,\varepsilon)$ is a non-increasing and concave function with R and $\eta PZ(R,\varepsilon)$ is a linear decreasing function with R, which is consistent with Theorem 1 and Theorem 2, respectively. It can be also seen that $\eta PW(R,\varepsilon)$ is always larger than $\eta PZ(R,\varepsilon)$, which verifies Theorem 3. In addition, it can be observed that the functions $\eta PW(R,\varepsilon)$ and $\eta PZ(R,\varepsilon)$ increase with P for a given robust outage capacity R, due to the following reasons: 1) Both functions $\eta PW(R,\varepsilon)$ and $\eta PZ(R,\varepsilon)$ include P in their multiplication expressions; 2) From (10) and (11), a larger P leads to a larger feasible region of Problem 3 and Problem 4, and thus larger $W(R,\varepsilon)$ and $Z(R,\varepsilon)$, respectively.

Fig. 2 illustrates how $\eta PW(R,\varepsilon)$ and $\eta PZ(R,\varepsilon)$ vary with outage probability ε under different robust outage capacity R. It shows that both $\eta PW(R,\varepsilon)$ and $\eta PZ(R,\varepsilon)$ grow when ε increases, which is consistent with Theorem 1 and Theorem 2, respectively. This is because when ε increases, the feasible region of α in Problem 3 and β in Problem 4 are larger, according to (10) and (11), respectively. It is also observed that when ε increases, $\eta PW(R,\varepsilon)$ and $\eta PZ(R,\varepsilon)$ increase fast in small ε region, and increase slowly in large ε region. This is because when ε increases, the term $\sqrt{\left(\frac{1}{\varepsilon}\right)-1}$ in constraints (10) and (11) decreases fast in small ε region, and decreases slowly in large ε region.

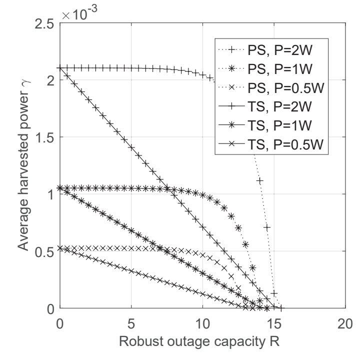

Fig. 1. Average harvested power versus robust outage capacity.

To demonstrate the impact of energy harvesting, Fig. 3 shows how $\eta PW(R,\varepsilon)$ and $\eta PZ(R,\varepsilon)$ vary with energy conversion efficiency η under different robust outage capacity R. When energy conversion efficiency η grows from 0.3 to 0.5, the average harvested power grows, which is intuitive.

Fig. 3 also shows the impact of energy harvesting nonlinearity. For a nonlinear energy harvester, the output denoted E_O is given [10, eq. (2)] as $E_O = \left(\frac{M}{(1+e^{-a(E_I-b)})} - \frac{M}{(1+e^{ab})}\right) / \left(1 - \frac{1}{(1+e^{ab})}\right)$ where E_I is the harvester's received power, M is the saturation power (the maximal output of the energy harvester), and a and b are parameters for the nonlinearity. Here we follow the same setting as in [10]: $a = 1500, b = 0.0022$. Similar to Section III-A, we can formulate optimization problems that maximize harvested power given R_p under PS scheme and given R_t under TS scheme, and transform the formulated problems to convex ones. Fig. 3 shows that, with a higher saturation power M, more average harvested power is achieved.

Fig. 4 shows average harvested power versus achievable capacity in our method (using legend "robust") and the method in [4], [5] that measures instantaneous CSI and solves an optimization problem to get the optimal PS/TS ratio configuration in every fading block (using legend "full CSI"). The method with full CSI can achieve a not-significant performance gain over our method, which is because more channel information is utilized.[7] However, our method has significant advantages in communication overhead (we do not need to estimate instantaneous CSI in every fading block), computation overhead (we do not need to solve an optimization problem in every fading block), and complexity (we do not need to configure the PS/TS ratio in every fading block).

V. Conclusion and Further Discussion

We have studied the rate-energy tradeoff for a SIMO SWIPT system under PS and TS schemes with only information of mean and covariance matrix of the channel. Our target is to maximize the average harvested power for a given robust outage capacity. We have transformed the formulated optimization problems to convex ones. We have proved the convexity of robust outage

[7]The performance of the method with full CSI shown in Fig. 4 does not include the impact of communication overhead that is needed to obtain instantaneous CSI. If communication overhead is taken into account, the achieved capacity should be lower.

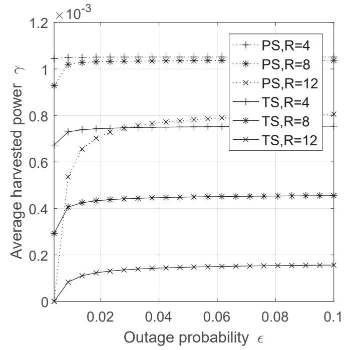

Fig. 2. Average harvested power versus outage probability.

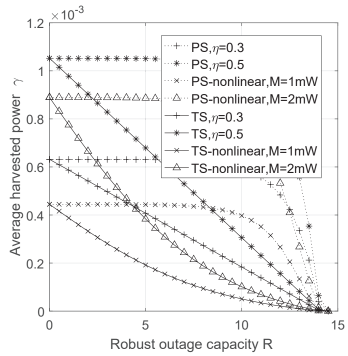

Fig. 3. Impact of energy conversion efficiency and energy harvesting nonlinearity.

capacity-energy region under PS and TS schemes. We have also proved that the PS scheme outperforms the TS scheme.

In this research, we have investigated a single transmitter-receiver pair. When multiple transmitter-receiver pairs are active simultaneously, the mutual interference among the multiple pairs will impair the information decoding (negative effect), but can also help the receivers to harvest more energy (positive effect). The tradeoff between the positive and negative effects should be taken into account.

REFERENCES

[1] X. Lu, P. Wang, D. Niyato, D. I. Kim, and Z. Han, “Wireless networks with RF energy harvesting: A contemporary survey,” *IEEE Commun. Surveys Tuts.*, vol. 17, no. 2, pp. 757-789, Second Quarter, 2015.

[2] X. Zhou, R. Zhang, and C. K. Ho, “Wireless information and power transfer: Architecture design and rate-energy tradeoff,” *IEEE Trans. Commun.*, vol. 61, no. 11, pp. 4754-4767, Nov. 2013.

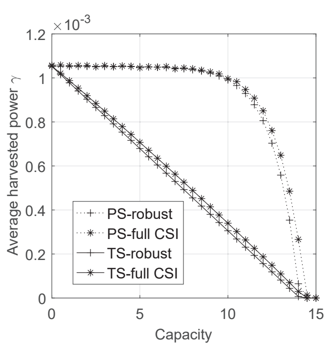

Fig. 4. Comparison of our method with existing methods.

[3] X. Zhou, “Training-based SWIPT: Optimal power splitting at the receiver,” *IEEE Trans. Veh. Technol.*, vol. 64, no. 9, pp. 4377-4382, Sep. 2015.

[4] L. Liu, R. Zhang, and K. C. Chua, “Wireless information transfer with opportunistic energy harvesting.” *IEEE Trans. Wireless Commun.*, vol. 12, no. 1, pp. 288-300, Jan. 2013.

[5] L. Liu, R. Zhang, and K. C. Chua, “Wireless information and power transfer: A dynamic power splitting approach,” *IEEE Trans. Commun.*, vol. 61, no. 9, pp. 3990-4001, Sept. 2013.

[6] I. M. Kim and D. I. Kim, “Wireless information and power transfer: Rate-energy tradeoff for equi-probable arbitrary-shaped discrete inputs,” *IEEE Trans. Wireless Commun.*, vol. 15, no. 6, pp. 4393-4407, June 2016.

[7] S. Li, W. Xu, Z. Liu, and J. Lin, “Independent power splitting for interference-corrupted SIMO SWIPT systems,” *IEEE Commun. Lett.*, vol. 20, no. 3, pp. 478-481, Mar. 2016.

[8] R. Zhang and C. K. Ho, “MIMO broadcasting for simultaneous wireless information and power transfer,” *IEEE Trans. Wireless Commun.*, vol. 12, no. 5, pp. 1989-2001, May 2013.

[9] X. Zhu, W. Zeng, and C. Xiao, “Precoder design for simultaneous wireless information and power transfer systems with finite-alphabet inputs,” *IEEE Trans. Veh. Technol.*, vol. 66, no. 10, pp. 9085-9097, Oct. 2017.

[10] K. Xiong, B. Wang, and K. J. R. Liu, “Rate-energy region of SWIPT for MIMO broadcasting under nonlinear energy Harvesting Model,” *IEEE Trans. Wireless Commun.*, vol. 16, no. 8, pp. 5147-5161, Aug. 2017.

[11] M. Chynonova, “Multiuser scheduling for simultaneous wireless information and power transfer system,” M.S. thesis, Friedrich-Alexander University Erlangen-Nürnberg, Germany, 2015.

[12] A. Ben-Tal, L. E. Ghaoui, and A. Nemirovski, *Robust Optimization*. Princeton: Princeton University Press, 2009.

[13] D. Tse and P. Viswanath, *Fundamentals of Wireless Communication*. Cambridge University Press, 2005.

[14] D. Bertsimas and I. Popescu, “Optimal inequalities in probability theory: A convex optimization approach,” *SIAM J. Optimization*, vol. 15, no. 3, pp. 780-804, 2005.